Dimensions of Plectonemically Supercoiled DNA

Svetlana S. Zakharova,* Wim Jesse,* Claude Backendorf,* Stefan U. Egelhaaf,† Alain Lapp,‡ and Johan R. C. van der Maarel*

*Leiden Institute of Chemistry, Leiden University, 2300 RA Leiden, The Netherlands; †Department of Physics and Astronomy, University of Edinburgh, Edinburgh EH9 3JZ, United Kingdom; and ‡Laboratoire Léon Brillouin, CE de Saclay, 91191 Gif-sur-Yvette Cedex, France

ABSTRACT With a view to determine the configuration and regularity of plectonemically supercoiled DNA, we have measured the small angle neutron scattering from pUC18 plasmid in saline solutions. Furthermore, we have derived the mathematical expression for the single chain scattering function (form factor) of a superhelical structure, including the longitudinal and transverse interference over the plectonemic pitch and radius, respectively. It was found that an interwound configuration describes the data well, provided interactions among supercoils are accounted for in the second virial approximation. The opening angle was observed to be relatively constant and close to 58°, but it was necessary to include a significant distribution in radius and pitch. For diluted supercoils with vanishing mutual interaction, the derived structural results agree with independent measurements, including the distribution in linking number deficit as determined by gel electrophoresis. With increasing plasmid concentration, prior and covering the transition to the liquid-crystalline phase, the radius and pitch are seen to decrease significantly. The latter observation shows that compaction of negatively supercoiled DNA by confinement results in a decrease in writhing number at the cost of a positive twist exerted on the DNA duplex. It is our conjecture that the free energy associated with this excess twist is of paramount importance in controlling the critical boundaries pertaining to the transition to the anisotropic, liquid-crystalline phase.

INTRODUCTION

Closed circular DNA usually exists in a supercoiled, plectonemic configuration in which the DNA duplex is wound around another part of the same molecule to form a higher order helix. The plectonemic negative supercoiling, with a right-handed interwinding, is the most likely conformation present in vivo. The excess free energy associated with the supercoiling is used in many cellular mechanisms. Examples include the replication and transcription of DNA, the formation of nucleosomes and other protein complexes on DNA, and the formation of altered DNA structures such as cruciforms (Bates and Maxwell, 1993). Apart from the importance in understanding the mechanisms involved in vivo, the interplay between conformation and interactions in topologically constrained polymers is of interest in its own right from a biophysical point of view.

With the advent of high-resolution (cryo-) electron microscopy (Boles et al., 1990; Bednar et al., 1994) and atomic force microscopy (Rippe et al., 1997; Lyubchenko and Shlyakhtenko, 1997; Cherny and Jovin, 2001), the supercoils can be directly visualized. In these studies the plectonemic parameters, i.e., radius, pitch, opening angle, and length projected on the superhelical axis were obtained as a function of superhelical density and/or supporting electrolyte concentration. The main observation is that the shape of the interwound superhelix is generally quite irregular, but the average radius is inversely proportional with the superhelical density and decreases with increasing ionic strength of the supporting medium. However, these visualization techniques are never without some ambiguity. First, it is difficult to preserve the ionic conditions during the elaborate sample preparation procedures and there is always a possible effect of the spreading interface on the molecular conformation (Fujimoto and Schurr, 2002). Furthermore, apart from cryo-electron microscopy, these interfacial techniques are not well adopted to investigate typical three-dimensional solution properties such as plasmid excluded volume effects and crowding. Accordingly, it is desirable to perform bulk radiation scattering experiments to infer the structure of the supercoils close to their native state.

Scattering work on supercoiled DNA is scarce. Early work using low angle x-ray scattering shows rather featureless structure factors, which were interpreted with a toroidal molecular configuration (Brady et al., 1983, 1987). This observation is at odds with the images obtained with modern high-resolution microscopy techniques, which show clearly plectonemic, interwound molecular conformations. The interwound structure has also been observed in more recent small angle neutron scattering (SANS) work on supercoiled DNA either in dilute solution (Hammermann et al., 1998) or in liquid-crystalline environment (Torbet and DiCapua, 1989). From the scaling of the interaction peak position (Bragg spacing) with plasmid concentration, the latter authors obtained a pitch angle $36 \pm 5°$ for concentrations above 45 g of DNA/dm^3. With the linking number deficit determined with gel electrophoresis, they further derived a radius $r = 8 \pm 1$ nm and a pitch $2\pi p = 36 \pm 4$ nm. With a similar procedure as in the present contribution, Hammermann et al. (1998) obtained significantly smaller

Submitted December 17, 2001 and accepted for publication April 17, 2002.

Address reprint request to Dr. Johan R. C. van der Maarel, Gorlaeus Laboratories, Leiden University, P. O. Box 9502, 2300 RA Leiden, The Netherlands. Tel.: 31-71-5274543; Fax: 31-71-5274397; E-mail: j.maarel@chem.leidenuniv.nl.

© 2002 by the Biophysical Society

0006-3495/02/08/1106/13 $2.00

values for the radius of the superhelix of pUC18 bacterial plasmid (2686 bp). In these previous scattering works, attempts to observe interference over the superhelical pitch were unsuccessful. As we will see shortly, this is mainly because of the existence of a rather broad distribution of topoisomers in a typical DNA preparation.

Supercoiling is also of paramount importance in controlling the formation of a liquid crystal, through the effect of the plectonemic dimensions and possible branching of the superhelix on the excluded volume. The key issue how spatial confinement controls the radius, pitch, and associated excess free energy has not been addressed yet. Accordingly, we thought it useful to focus on the dimensions of the supercoil as a function of plasmid concentration in a range prior and covering the transition to the liquid crystalline phase. For this purpose, we will first derive a mathematical expression for the total scattering function, including interactions among supercoils in the second virial approximation. This expression should include both longitudinal and transverse interference over the pitch and radius, respectively. Furthermore, it will be necessary to include a variation in the molecular shape due to the presence of a distribution in linking number deficit, thermal fluctuations, and/or, in the case of biphasic samples, partitioning over coexisting anisotropic and isotropic phases. From a comparison with our SANS data from pUC18 plasmid in saline solutions, we will estimate the regularity of the superhelical structure and the extent to which the configuration follows locally the classical path. The derived results for the radius, pitch, and opening angle will than be compared with the corresponding literature values obtained with microscopic visualization techniques. Finally, we will discuss the observed concentration dependence of the number of superhelical turns in terms of spatial confinement effects.

THEORY

Topology

For a description of the topology, it is assumed that the double-stranded DNA coil takes a helical configuration that is well defined locally at a length scale on the order of the radius r and the pitch $2\pi p$ (Fig. 1). We let the helix be right-handed with a negative superhelical density $\sigma = \Delta Lk\,/Lk_0$, with excess linking number deficit ΔLk and Lk_0 being the linking number if the coil is fully relaxed. The excess linking number deficit is related to the writhing number Wr and the excess twist ΔTw according to

$$\Delta Lk = Wr + \Delta Tw \tag{1}$$

(White, 1969). For a right-handed, regular supercoil without end loops, the writhing number is simply proportional to the number of crossings n when viewed perpendicular to the superhelical axis $Wr = -n\sin\alpha$, with the plectonemic pitch angle α as in Fig. 1 (Bloomfield et al., 2000). L denotes the total length of the supercoil projected on the superhelical axis. It is convenient to define the normalized length $2L/l$, with l being the DNA length measured along the contour. From integration along the contour, it follows that

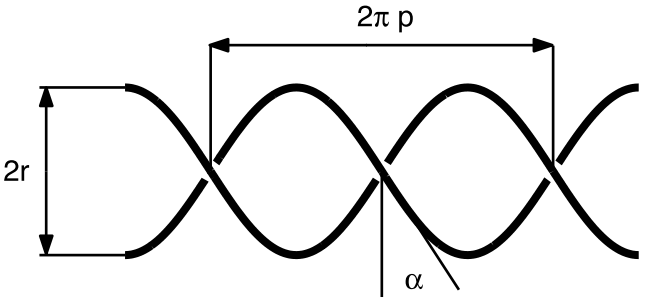

FIGURE 1 Local configuration of the plectonemic helix with radius r, pitch p, and opening angle α.

$$2L/l = p/(p^2 + r^2)^{1/2} \tag{2}$$

if the end loops are neglected. The pitch angle α is given by

$$\tan\alpha = p/r = (2L/l)/(1 - (2L/l)^2)^{1/2} \tag{3}$$

and the writhing number reads

$$Wr = -lp/(2\pi(p^2 + r^2)) \tag{4}$$

The local structure of the plectoneme is fully characterized by the lengths p and r. These two parameters determine the opening angle α, the writhe Wr, and the normalized length of the superhelical axis $2L/l$.

For an interpretation of the data, it is necessary to calculate the contribution to the scattering from a single DNA molecule. This single chain contribution, which is commonly referred to as the form factor, is completely defined by the topology of the supercoil and can be expressed in terms of p, r, and L. Once the form factor is known, interactions among different supercoils can be included in the description of the total structure factor in the random phase approximation as detailed below.

Form factor

At a larger length scale on the order of the plectonemic length L, the supercoil can branch. In the interpretation of our scattering experiments, branching effects are unimportant however. This is because the momentum transfer range q (defined by the wavelength λ of the radiation and the angle θ between the incident and scattered beam according to $q = 4\pi/\lambda\sin(\theta/2)$) exceeds L^{-1} by at least an order of magnitude and the scattering is particularly sensitive to interference over a spatial extent on the order of the plectonemic radius and pitch ($qL \gg 1$). We will accordingly neglect branching in the calculation of the form factor. Furthermore, we will also ignore the scattering contributions due to the end loops and the effects of overall

flexibility of the superhelical axis. The error in the form factor introduced by the neglect of the end loops becomes less significant for supercoils with higher superhelical density. The effects of flexibility are minimal for $qL_s \gg 1$ with L_s the bending persistence length of the supercoil (~100 nm, i.e., being twice the value of the persistence length of the duplex L_p). For the time being, we will also neglect the effect of the radius of gyration r_p of the cross-section of the double-stranded DNA duplex. The latter effect is important only for very high values of momentum transfer where $qr_p \approx 1$ and can easily be taken into account once the form factor of the superhelix is known.

Before engaging in any detailed calculation, it is interesting to gauge the limiting behavior of the single chain scattering function for low and high values of momentum transfer, respectively. In the low q range, with $qr \ll 1$ and $qp \ll 1$, the details of the plectonemic structure (i.e., radius and pitch) are beyond observation. At this rather extended distance scale, but at lengths significantly smaller than L ($qL \gg 1$), the supercoil is seen as a rodlike object with form factor $P(q) = \pi/(qL)$ (overall flexibility of the superhelical axis is ignored). At higher values of momentum transfer in the range $qr \gg 1$ and $qp \gg 1$, the scattering is essentially given by a single strand of the superhelix (not to be confused by a single strand of the DNA duplex). The high q limiting form of the form factor of a single DNA duplex is $P(q) = \pi/(ql)$, with l the DNA contour length (here, the finite cross section of the duplex is ignored). In both regimes, the form factor shows the characteristic q^{-1} scaling for rodlike particles (Higgins and Benoit, 1994). With increasing value of momentum transfer, the prefactor drops, however, from the DNA density per unit plectonemic length L^{-1} to the density per unit contour length l^{-1}. The ratio of the prefactors gives, hence, l/L, which is particularly promising from an experimental point of view. It is clear that a full description should agree with these two limiting situations. As we will see shortly, the form factor is particularly rich in information concerning the plectonemic structure in the intermediate q range with $qr \approx 1$ and $qp \approx 1$.

The exact form factor pertaining to a regular plectonemic structure is derived in the appendix and reads

$$P(q) = \int_0^1 d\mu \left(\left[\frac{\sin(q\mu L/2)}{(q\mu L/2)} \right]^2 J_0^2(qr(1-\mu^2)^{1/2}) + \sum_{k=1}^{\infty} \left(\left[\frac{\sin((q\mu + 2k/p)L/2)}{(q\mu + 2k/p)L/2} \right]^2 + \left[\frac{\sin((q\mu - 2k/p)L/2)}{(q\mu - 2k/p)L/2} \right]^2 \right) J_{2k}^2(qr(1-\mu^2)^{1/2}) \right) \quad (5)$$

with J_k being the Bessel functions of integer order. The restriction to the even $2k$ terms comes from the fact that the contributions of the two opposing strands in the superhelix have been averaged. The form factor is normalized to unity at $q = 0$. As anticipated, the structure is fully described by the lengths p, r, and L. In the relevant momentum transfer range $qL \gg 1$, the integration over orientation variable μ can be done analytically. In this range of momentum transfer, the form factor takes the relatively simple approximate form

$$P(q) = \frac{\pi}{qL} \left[J_0^2(qr) + 2 \sum_{k=1}^{qp/2} J_{2k}^2((q^2 - 4k^2/p^2)^{1/2} r) \right], \quad qL \gg 1 \quad (6)$$

in which the summation is restricted to those terms with index $k < qp/2$. The high q approximate solution of the single chain scattering function is sensitive to the DNA density per unit length projected on the superhelical axis L^{-1}. In the derivation of these expressions, the effect of the radius of gyration r_p of the cross-section of the DNA duplex has been ignored. Because of the difference in length scales, this effect can be taken into account by multiplication of the form factor of the superhelix Eqs. 5 or 6 with the one pertaining to the cross-section

$$P_c(q) = [2J_1(qr_p)/(qr_p)]^2 \quad (7)$$

(van der Maarel, 1999; Zakharova et al., 1999).

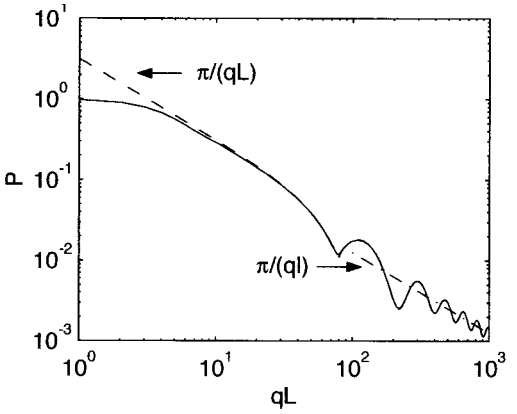

FIGURE 2 Form factor of a superhelix according to the exact (*solid line*) and approximate (*dashed line*) Eq. 5 and 6, respectively. The low and high q limiting behavior is given by $\pi/(qL)$ and $\pi/(ql)$ (*dashed-dotted line*), respectively. The parameters are the radius $r = 7$ nm, pitch $p = 9.3$ nm, and contour length $l = 920$ nm.

The exact and approximate expressions Eqs. 5 and 6, respectively, are compared in Fig. 2. The parameters are typical for pUC18 plasmid with a normalized plectonemic length $2L/l = 0.8$, which corresponds with an opening angle $\alpha = 53°$. The experimental value of the normalized length, deduced from electron microscopy, is found to be 0.82 ($\alpha = 55°$) and is constant within a margin 0.05 (Boles et al., 1990). For qL exceeding, say, 10, the exact and approximate expressions are indiscernible. Furthermore, the approximate solution has the right low and high q limiting behavior as already anticipated from our scaling arguments. In the in-

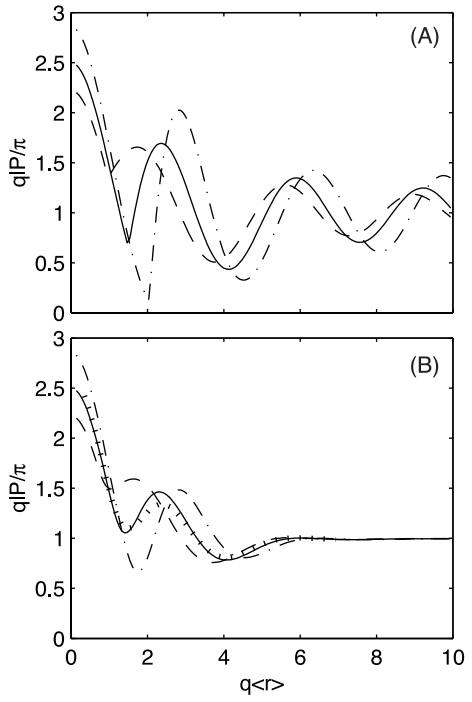

FIGURE 3 Normalized form factor qlP/π versus $q\langle r\rangle$ without (*A*) and with (*B*) 20% variation in the radius r ($r_m = 2$ nm). The lines refer to a normalized plectonemic length $2L/l = 0.7$ (*dashed-dotted*), 0.8 (*solid*), and 0.9 (*dashed*). The other parameters are as in Fig. 2. Except the dotted line in *B*, all curves are calculated with a fixed opening angle $\alpha = 44°$, 53°, and 64° for $2L/l = 0.7$, 0.8, and 0.9, respectively. The dotted line includes the effect of an additional 25% fluctuation in pitch about the average value set by the average opening angle $\alpha = 53°$ ($2L/l = 0.8$).

termediate q range, the form factor shows strong oscillatory behavior, which is due to intrasuperhelix interference both in the radial and longitudinal direction over lengths r and p, respectively. The intrasuperhelix interference is more clearly demonstrated if the form factor is normalized in a way that it goes to unity at high q.

Fig. 3 displays the normalized form factor qlP/π versus $q\langle r\rangle$. The form factor is calculated without as well as with fluctuations in molecular shape as detailed below. In the limit $q \to 0$, qlP/π extrapolates to two times the inverse normalized plectonemic length l/L. Apart from their obvious dependence on the average radius (r), the positions of the minimums and maximums in the normalized form factor are rather sensitive to the value of the normalized length (or, according to Eq. 3, the opening angle α). This sensitivity of the periodicity to the normalized length comes from longitudinal interference over the plectonemic pitch through the (pitch dependent) series of Bessel functions in Eqs. 5 or 6. The corresponding terms also ensure the correct high q limiting behavior. The first leading term $J_0^2(qr)$ is the form factor of a pair of point scatterers at a constant distance $2r$ and averaged over a circle. Restriction to this first term in the analysis of the scattering from a plectonemic structure, as has been done in previous scattering works (Brady et al., 1983, 1987; Hammermann et al., 1998), is clearly not sufficient for a precise estimate of the diameter of the superhelix.

As we will see shortly, our experimental results do not show such strong oscillatory behavior, because in reality there are fluctuations in the radius r, pitch p, and opening angle α. To include these fluctuations in our model, we assume a Gaussian distribution in r with a standard deviation σ_r and a distance of closest approach of the two opposing DNA strands in the superhelix $2r_m$. Here, and in subsequent calculations, the cut off radius r_m was set to 2 nm, being approximately the sum of the DNA duplex outer radius and a condensed counterion layer thickness. As a first approximation, we will also assume that α is constant. The latter assumption is supported by the electron microscopy observation of a constant normalized plectonemic length over a large range in superhelical density $-0.12 \lesssim \sigma \lesssim -0.02$ (Boles et al., 1990). The pitch p is hence proportional to r, with a proportionality factor given by the normalized length according to Eq. 3. Such a distribution in radius and pitch with constant opening angle can be envisioned due to the presence of a distribution of topoisomers with different linking number deficit in our DNA preparation (see below). As displayed in Fig. 3, a 20% fluctuation in r ($\sigma_r/r = 0.2$) is already sufficient to damp the oscillations to a significant degree. We have also allowed for an additional Gaussian broadening in pitch, which relates to a fluctuation in the opening angle α. As can be seen in Fig. 3, an additional 25% fluctuation in p ($\sigma_p/p = 0.25$) about the average value set by the average opening angle $\alpha = 53°$ ($2L/l = 0.8$) gives a minor effect only.

Total structure factor

Of course, the scattering does not only depend on the properties of a single DNA molecule but is also sensitive to interference among different supercoils. Doing experiments at low solute volume fractions minimizes the latter interference, but practical reasons, such as neutron beam intensity and scattering cross section, set a lower bound to the concentration range. In polyelectrolytes, including DNA, interchain structure at wavelengths on the order of the electrostatic screening length is notoriously difficult to describe (Nierlich et al., 1979; van der Maarel et al., 1992; Yethiraj and Shew, 1996; van der Maarel and Kassapidou, 1998). If the superhelix is modeled as a uniformly charged cylinder with radius r immersed in a medium with ionic strength I, its effective diameter can be calculated in the Debye-Hückel approximation and takes the form (Stigter, 1977; Fixman and Skolnick, 1978)

$$D_{\text{eff}} = 2r + \kappa^{-1}(\ln A' + \gamma + \ln 2 - 1/2)\,,$$
$$A' = A \exp(-2\kappa r) \qquad (8)$$

Here, γ denotes Euler's constant and the screening length κ^{-1} given by $\kappa^2 = 8\pi QI$, with Bjerrum length $Q = e^2/(\varepsilon kT)$. The constant $A = 2\pi\bar{\nu}_{\text{eff}}^2 Q\kappa^{-1}$ depends on the effective number of charges per unit length along the superheli-

cal axis $\bar{\nu}_{\text{eff}}$. If the charge is renormalized according to the Manning's (1969) condensation concept, $\bar{\nu}_{\text{eff}} = [Q\kappa r K_1(\kappa r)]^{-1}$, with K_1 the first order modified Bessel function of the second kind. In 0.05 M monovalent salt and with a bare diameter 20 nm (see below), the effective diameter of the superhelix amounts 21 nm. We have, hence, a sufficient amount of supporting low molecular weight electrolyte, so that the electrostatic interactions are screened within the range of the diameter of a single supercoil. Accordingly, the DNA molecules do not interact very strongly and the scattering behavior is anticipated to agree with virial theory. We will use the most simple random phase approximation (de Gennes, 1979; des Cloiseaux and Jannink, 1990) for the total structure factor

$$S(q) = NP(q)/(1 + 2A_2\rho P(q)) \quad (9)$$

with N the number of nucleic acid monomers per DNA molecule (i.e., two times the number of base pairs), A_2 the second virial coefficient, and ρ denotes the DNA concentration in number of plasmids per unit volume. Theoretical expressions for the second virial coefficient are available for, e.g., rigid rods including electrostatic interactions and end effects (Onsager, 1949; Odijk, 1990). However, due to various spurious effects such as branching and overall flexibility, we consider interpretation of the second virial coefficient of DNA supercoils with a rigid rod model not feasible and we will treat A_2 as an adjustable parameter.

MATERIALS AND METHODS

Isolation of pUC18 clone vector DNA

pUC18 plasmid (2686 bp) was prepared from *Escherichia coli* DH5α (Bhikhabhai et al., 2000). A colony was transformed with pUC18 and grown on a Luria Broth agar plate with ampicillin (100 μg/mL). A single colony was taken to grow a culture in Terrific Broth medium (12 g of tryptone, 24 g of yeast extract, 4 mL of glycerol, 2.3 g of KH_2PO_4, and 12.5 g of K_2HPO_4 per dm^3) and ampicillin at 37°C. After 7 h, this culture was put into a fermentor, which contained 30 dm^3 Terrific Broth-medium, ampicillin, and an antifoam agent. The bacteria were cultured for 17 h at 37°C under continuous shaking, aeration, and, subsequently, harvested and stored at −20°C. The cells were suspended in TEG buffer (25 mM Tris, 10 mM EDTA, 50 mM glucose, pH 8) and lysed with an alkaline solution (0.2 M NaOH, 1% sodium dodecyl sulfate) at room temperature. Bacterial genomic DNA, cellular debris, and proteins were precipitated by the addition of 3 M potassium acetate at 4°C. After centrifugation, the supernatant was treated with 5 M ammonium acetate to precipitate any residual contaminants (Sun et al., 1994). RNA and protein were removed with Rnase (20 μg/mL, 37°C, 1 h) and proteinase K (100 μg/mL, 55°C, 1 h) treatments, respectively. After precipitation with cold isopropanol, the DNA pellet was dried for a short period and dissolved in TE-buffer (10 mM Tris, 1 mM EDTA, pH 8) for storage at 4°C. The advantage of this procedure is that it has a high yield of typically 75 mg of plasmid DNA per isolation using 4 of 30 dm^3 cell culture.

Plasmid characterization, purification, and sample preparation

The integrity of the plasmid was checked with 1% agarose gel electrophoresis in Tris-acetate buffer (40 mM Tris-acetate, 2 mM EDTA, pH 8.3) at 75 V for 1 h (Backendorf et al., 1989). The linking number deficit and the percentage of open circular DNA were determined by 1.4% agarose gel electrophoresis in the same buffer but with 10 μg/mL chloroquine at 50 V for 17 h (van Workum et al., 1996). The results are displayed in Figs. 4 and 5, respectively. Apart from supercoiled DNA, an isolated batch contained some chromosomal DNA and a small amount of aggregated plasmid DNA. The density profile in Fig. 5 shows a rather broad topoisomer distribution with predominant linking number deficit −7 and deviation ±3 ($\Delta Lk = -7 \pm 3$), which corresponds with a superhelical density $\sigma = -0.03$ (for chloroquine-free pUC18 $Lk_0 = 262$). Furthermore, gel electrophoresis indicates that less than 5% of plasmids are nicked and open circular. The plasmids were further purified with fast performance liquid chromatography on a 40-mL bed volume Q-sepharose column (XK 26/20, Pharmacia BioTech, Uppsala, Sweden) (Prazeres et al., 1998). Gel electrophoresis shows that the purified material is now essentially free of open circular and/or linear plasmid, aggregated plasmid, and chromosomal DNA (Fig. 4). Furthermore, the ratio of the optical absorbencies $A_{260}/A_{280} = 1.83$ indicates that the material is also free of protein. The hypochromic effect at 260 nm (>35%) confirms the integrity of the duplex. For sample preparation, the purified plasmid was precipitated in ethanol and the 10% residual water content in the gently dried pellet was determined with infrared spectroscopy. The pellet was subsequently dissolved in 0.05 M NaCl, and the DNA con-

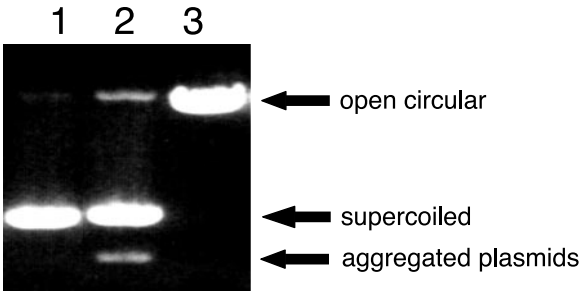

FIGURE 4 Analysis by agarose gel electrophoresis. (*Lane 1*) Fast performance liquid chromatography purified supercoiled material; (*lane 2*) nonpurified batch; (*lane 3*) open circular plasmid.

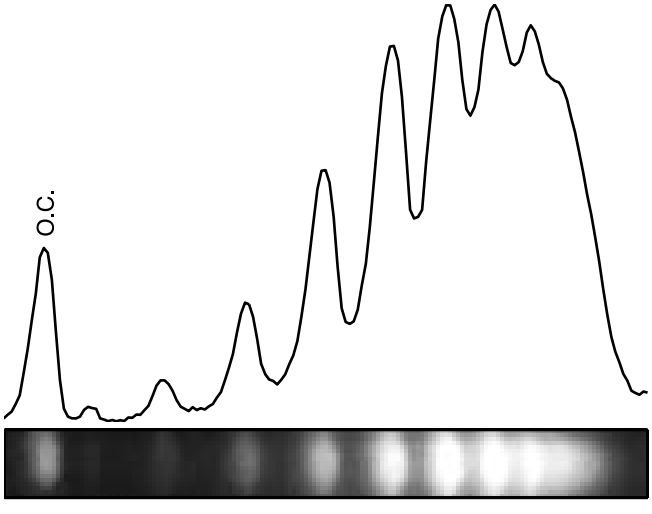

FIGURE 5 Topoisomer distribution in the nonpurified batch by agarose gel electrophoresis in the presence of chloroquine. The density profile shows <5% open circular plasmid and linking number deficit $\Delta Lk = -7 \pm 3$. Linking number deficits less than −9 are not resolved.

centration was determined by weight and checked with ultraviolet spectroscopy. Standard quartz cuvettes with 0.1-cm path length were used.

Scattering

Small angle neutron scattering experiments were done with the PAXY (test experiments only) and D22 diffractometers, situated on the cold sources of the high neutron flux reactors at the Laboratoire Léon Brillouin, CEN de Saclay, and Institute Max von Lauc - Paul Langevin respectively. The temperature was kept at 298 K. The reported data were collected with the D22 instrument in two different configurations. A wavelength of 0.7 nm was selected, and the effective distances between the sample and the planar square multidetector (sample-detector, (S-D) distance) were 2 and 8 m, respectively, with a 0.4-m detector offset for the 2-m S-D distance only. This allows for a momentum transfer range of 0.05 to 4 nm^{-1}. The counting times were approximately 2 h/sample, irrespective S-D distance. Data reduction allowed for sample transmission and detector efficiency. The efficiency of the detector was taken into account with the scattering of H_2O. Absolute intensities were obtained by reference to the attenuated direct beam and the scattering of the solvent H_2O was subtracted. Finally, the intensities were corrected for a small solute incoherent scattering contribution. In the present solutions, the scattering is dominated by the DNA structure, because the nucleotide scattering length contrast exceeds the corresponding values of the small ions by two orders of magnitude. The coherent part of the solvent subtracted SANS intensity gives hence the DNA structure factor according to $I(q) = \rho_m \bar{b}^2 S(q)$ with ρ_m the DNA concentration in number of nucleotides per unit volume ($\rho_m = N\rho$). The contrast $\bar{b} = 11.4 \times 10^{-12}$ cm has been calculated according to the pUC18 base composition A:G:C:T = 0.245:0.252:0.255:0.248 (NCBI database, accession number L08752) and the nucleotide scattering lengths reported by Jacrot (1976).

RESULTS AND DISCUSSION

Scattering experiments were done on samples with plasmid concentration in the range 2 to 27 g of DNA/dm^3 in 0.05 M NaCl. This concentration range is just below and covering the transition to a liquid crystal (Torbet and DiCapua, 1989; Reich et al., 1994). The experimental results are displayed in Fig. 6, together with the theoretical structure factors of a plectonemic model and interactions in the second virial approximation. The result obtained from 2 g of DNA/dm^3 is not shown, because it is very similar to the one with 3 g/dm^3 plasmid concentration. This agreement shows that the effect of interactions among supercoils on the structure factor is vanishing small for DNA concentrations less than, say, 3 g/dm^3 (i.e., $\rho A_2 \approx 0$). For the samples with higher plasmid concentration, progressive interactions among supercoils results in a suppression of the intensity at longer wavelengths (smaller q values). Furthermore, the samples with 11 and 27 g/dm^3 plasmid concentration show an upturn for very low values of momentum transfer $q < 0.1$ nm^{-1}, which is not accounted for by the theoretical predictions. If the plasmid concentration exceeds 3 g/dm^3, the translucent samples exhibit birefringent domains when observed through crossed polarizers and a solid-like broadening of the ^{31}P resonance in the nuclear magnetic resonance spectrum. These observations comply with the progressive growth of liquid crystalline germs in an otherwise isotropic medium. The samples with 2 and 3 g of DNA/dm^3 are completely isotropic; the ones with 6 and 11 g of DNA/dm^3 are in the biphasic regime, and the sample with 27 g of DNA/dm^3 is completely liquid crystalline. The critical boundaries and the characteristics of the liquid-crystalline phase are, however, beyond the scope of the present paper and will be reported in an accompanying paper. Here, we focus on the concomitant effects of the compaction on the dimensions of the supercoil by a full analysis of the structure factor.

As displayed in Fig. 6, there is nice agreement with the theoretical predictions according to Eq. 9. We have used the approximate form factor expression Eq. 6, because $qL > 20$ in our experimental range of momentum transfer. The structure factors do not exhibit a significant intermolecular interaction peak. The agreement with second virial theory and the absence of an interaction peak indicate that the supercoils do not interact too strongly and that the ionic strength is sufficiently high to screen the electrostatic interactions over a relatively short range on the order of the plectonemic diameter. Due to the presence of a significant distribution in plectonemic radius and pitch, the structure factors do not exhibit strong oscillatory behavior. They do show, however, the anticipated q^{-1} scaling and the drop in prefactor from the inverse plectonemic length L^{-1} to the inverse contour length l^{-1} with increasing value of momentum transfer. The determination of the plectonemic dimensions will be further discussed below, once the structure factors are normalized to their high q limiting behavior. For q exceeding, say, 1 nm^{-1}, the structure factors show the characteristic deviation from q^{-1} scaling related to the finite cross-section of the DNA duplex. A fit of the relevant form factor Eq. 7 gives a radius of gyration $r_p = 0.8$ nm. This value agrees with the cross-section of the DNA duplex in the *B*-form. It is a little less than the outer radius 1 nm, due to the relatively open duplex structure related to the existence of grooves (van der Maarel et al., 1992; Zakharova et al., 1999).

The plectonemic structure is most clearly demonstrated in Fig. 7, where the structure factors are normalized in a way that they go to unity at high q. For this purpose, the structure factors are multiplied with q times the contour length l and divided by π times the number of nucleotides per plasmid N. For the sake of completeness, the data are also divided by the form factor pertaining to the cross-section of the duplex P_c, although the latter factor deviates little from unity in the relevant range $q <$ 1 nm^{-1}. The normalized structure factor extrapolates to two times the inverse normalized plectonemic length l/L for $q \to 0$ and in the absence of interactions. Due to the distribution in radius and pitch, the higher order oscillations are damped and the first oscillation takes the form of a shoulder (see Fig. 3). With increasing DNA concentration, this shoulder shifts to higher values of momentum transfer with a concomitant suppression at longer wavelengths due to progressive interactions among the supercoils. The deviations observed at very low q values ($q < 0.1$ nm^{-1}) comply with the existence of a long-range inhomogeneity in DNA density, possibly related to the existence of aggregated plasmid and/or the formation of crys-

talline spherulites (see accompanying paper). The shift of the shoulder and subsequent minimum toward higher values of momentum transfer with increasing plasmid concentration is related to a concomitant decrease in the average plectonemic pitch and radius. These observations will be further substantiated with the results of the fit procedure of the theoretical structure factor.

As discussed in the theoretical section, in the data analysis we neglect the contribution originating from the end loops as well as branching. Flexibility effects on the scattering function of a wormlike chain are less than 5% for our lower bound $qL_s \approx 2.5$ (with the bending persistence length of the supercoil $L_s \approx 100$ nm) and become negligible as q is increased (Norisuye et al., 1978). Accordingly, we expect that overall flexibility effects on the scattering from a supercoil are modest in the present q range.

The main contribution to the distribution in radius comes from the presence of a distribution in topoisomers with different linking number deficit as shown by gel electrophoresis (Fig. 5). Another source for a variation in radius is thermal fluctuations, as suggested by, e.g., analytical theory (Marko and Siggia, 1995; Ubbink and Odijk, 1999) and computer simulations (Gebe et al., 1996; Hammermann et al., 1998; Klenin et al., 1998). Furthermore, the partitioning of DNA over coexisting isotropic and liquid crystalline phases with a concomitant change in plectonemic dimensions contributes to a broadening of the distribution in radius. Of course, the opening angle can also fluctuate, but we assume that it takes a constant value. This assumption is supported by the observation of a constant normalized plectonemic length over a large range in superhelical density $-0.12 \lesssim \sigma \lesssim -0.02$ (Boles et al., 1990). Alternatively, the variation in pitch may be assumed uncorrelated with the variation in radius, but it was checked that such model gives an inferior fit (results not shown). The input parameters for our model are, hence, the plectonemic radius r, its distribution width σ_r, the opening angle α, and the second virial coefficient A_2 (ρA_2 was set to zero for the 3 g of DNA/dm^3 sample). The pitch p, the writhing number Wr, and the normalized plectonemic length $2L/l$ can subsequently be derived with Eq. 3. Estimation of the distribution widths in the latter parameters was done with standard variance propagation of the optimized variation in radius. The cut off radius pertaining to the distance of closest approach of the two DNA strands was set to $r_m = 2$ nm, being approximately the sum of the DNA duplex radius and the condensed counterion layer thickness. It was checked that a 25% variation in the latter value has no significant effect on the fitted parameters. The results are collected in Table 1. Note that the margins do not refer to error in the physical measurements, but rather to variation in the molecular shape resulting from the distribution in linking number deficit and/or thermal fluctuations.

In the diluted regime, the plectonemic radius takes a relatively large value $r = 10 \pm 4$ nm, and the supercoils are rather expanded with a solvent and small ions filled

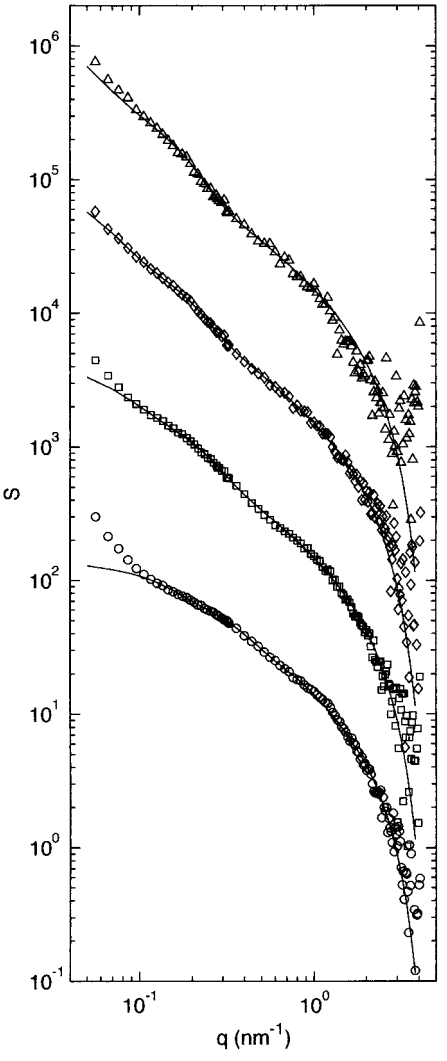

FIGURE 6 Structure factor S versus momentum transfer q in the double logarithmic representation. The DNA concentration is 3 (△), 6 (◇), 11 (□) and 27 (○) g/dm^3. The solid lines are calculated according to the theoretical structure factor with the adjusted parameters in Table 1. To avoid overlap, the data are shifted along the y axis with a multiplicative constant.

core spanning ~10 times the duplex diameter. This value, which is derived under solution conditions, is in good agreement with the electron microscopy result for DNA with a superhelical density $\sigma \approx -0.03$ in 0.105 M monovalent salt (Boles et al., 1990). The spreading of the supercoils on the electron microscopy grid has apparently no significant effect on the derived dimensions. There is also nice agreement with the SANS result of Torbet and DiCapua (1989), who obtained a 8-nm radius from the scaling of the position of the interaction peak in the liquid-crystalline regime above 45 g of DNA/dm^3 ($\sigma \approx -0.05$). With a similar experimental procedure as described in the present work, Hammermann et al. (1998) reported a significantly smaller radius 5.5 nm for pUC18

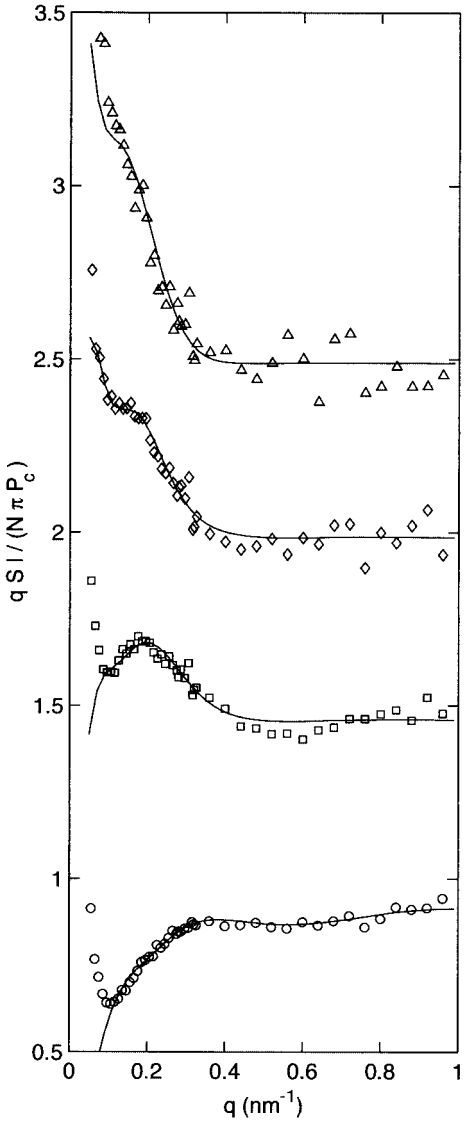

FIGURE 7 Normalized structure factor $qlS/(N\pi P_c)$ versus momentum transfer q. The concentrations and solid lines are as in Fig. 6. To avoid overlap, the data are incrementally shifted along the y axis with 0.5 units.

in 0.05 M NaCl. However, the latter authors did not take into account the longitudinal interference over the pitch (and, hence, they did not derive the opening angle), which has an important effect on the structure factor. From the results in Fig. 3 *b* and the position of the first minimum in the term $J_0^2(qr)$, we can estimate that the position of the minimum in the normalized structure factor is shifted by a factor, say, 1.7 towards higher values of momentum transfer once the longitudinal interference is included. If we tentatively scale Hammermann et al.'s result with this factor, we obtain a 9-nm, plectonemic radius which is in reasonable agreement with our result. There is also nice agreement with the value predicted by electrostatic theory within the Poisson-Boltzmann approximation (Marko and Siggia, 1995; Ubbink and Odijk, 1999).

TABLE 1 Parameters resulting from the fit of the structure factor to the scattering data*

c (g/dm^3)	r (nm)	p (nm)	α (°)	$2L/l$	Wr	A_2 (10^6 nm^3)
3	10 ± 4	21 ± 9	65	0.91	-6 ± 3	$-^{\dagger}$
6	9 ± 5	14 ± 7	57	0.84	-7 ± 4	0.55
11	8 ± 4	13 ± 7	59	0.86	-9 ± 5	1.22
27	5 ± 3	6 ± 4	52	0.79	-14 ± 10	1.92

*Fitted are the radius r, its distribution width σ_r, the opening angle α, and the second virial coefficient A_2 (r_m = 2 nm). The other parameters are derived through Eq. 3 and standard variance propagation.
$^{\dagger}\rho A_2$ is set to zero for the 3 g of DNA/dm^3 sample. Note that the margins refer to a variation in molecular shape resulting from the distribution in ΔLk and/or thermal fluctuations.

For diluted supercoils with vanishing mutual interaction, the derived values of the normalized length and the opening angle are also close to the electron microscopy values reported by Boles et al. (1990). These authors found an average normalized length 0.82 with a margin 0.05, which corresponds to an opening angle $\alpha = 55°$. For DNA in solution, we obtain $2L/l = 0.91$ and $\alpha = 65°$. The opening angle is very close to $63 \pm 20°$, reported for the superhelical regions in p1868 plasmids in air or hydrated in water and obtained with scanning force microscopy in the presence of $MgCl_2$ (Rippe et al., 1997). There is also nice agreement with the experimental value $62 \pm 5°$, obtained with the same technique for pPGM1 (2987 bp, $\sigma \approx -0.06$) plasmid in 0.05 M NaCl (Cherny and Jovin, 2001). With the optimized radius and pitch, the writhing number takes the value $Wr = -6 \pm 3$. With linking number deficit $\Delta Lk = -7 \pm 3$ (see Materials and Methods section), we derive a writhe per added link $Wr/\Delta Lk = 0.85$. Boles et al. (1990) reported a slightly smaller value $Wr/\Delta Lk. = 0.72$, but in view of the variation set by the distribution in radius and the neglect of end loops in our calculation of the writhe, we consider the agreement gratifying. Furthermore, the variation in writhe agrees with the variation in linking number deficit as observed by gel electrophoresis. This agreement indicates that the main contribution to the variation in adjusted parameters comes from the presence of a distribution of topoisomers rather than thermal fluctuations. To gauge the relative weight of the latter contribution, however, it is necessary to prepare plasmid with a narrow distribution in (preset) linking number deficit in sufficient quantities.

With increasing plasmid concentration, both the radius and pitch are seen to decrease significantly. Although the experiments were done with a constant concentration of added salt, the ionic strength increases from 0.05 to, say, 0.06 M, due to the uncondensed fraction 0.24 of counterions coming from the DNA (Manning, 1969). A decrease in radius with increasing ionic strength was previously observed with cryoelectron microscopy (Bednar et al., 1994), atomic force microscopy *in situ* (Lyub-

chenko and Shlyakhtenko, 1997), sedimentation and catenation experiments (Rybenkov et al., 1997a,b), SANS (Hammermann et al., 1998), as well as computer simulations (Gebe et al., 1996; Klenin et al., 1998). However, our increase in ionic strength comes from free counterions only and is so small that we consider spatial confinement effects of entropic origin of greater importance. This is also supported by the fact that the electrostatic interactions are screened over a distance on the order of 8 nm (as derived from the Poisson-Boltzmann equation for cylindrical polyelectrolytes in excess 0.05 M NaCl), which is well within the range of the superhelical diameter (10–20 nm).

As will be reported in an accompanying paper, in the present concentration range a first-order phase transition occurs to a liquid crystal. Except for the isotropic solutions with 2 and 3 g DNA/dm^3, our samples are microphase separated with a progressive growth of the liquid crystalline domains with increasing concentration. In the liquid crystalline 27 g of DNA/dm^3 sample, the spacing R between the molecules can be obtained from the hexagonal unit cell volume $\sqrt{3}R^2L/2 = \rho^{-1}$ and takes the value 13 nm. This spacing is on the same order of magnitude as the effective diameter of the supercoil 11.5 nm, as derived from the linearized Poisson-Boltzmann equation according to Eq. 8 with bare diameter 10 nm (Table 1) and in 0.05 M monovalent salt. To accommodate the molecules in the confined state, the radius of the supercoil has to decrease at the cost of a significant elastic bending and twisting energy of the duplex.

As anticipated, the normalized length and opening angle do not change much, although there is a tendency to smaller values for higher DNA concentrations. In this context, it is of interest to note that Torbet and DiCapua (1989) reported a pitch angle 36 ± 5° in the liquid crystalline regime for plasmid concentrations above 45 g/dm^3. This decrease in pitch angle and normalized length shows that, apart from a decrease in diameter, spatial confinement results in a slight compression of the supercoil in the longitudinal direction. On the other hand, the values averaged over the various DNA concentrations in Table 1, $2L/l = 0.85 \pm 0.05$ and $\alpha = 58 \pm 5°$, are very close to the ones obtained from electron microscopy: $2L/l = 0.82 \pm 0.05$ and $\alpha = 55°$ (Boles et al. 1990) and theoretical analysis $2L/l = 0.81$ and $\alpha = 54°$ (Ubbink and Odijk, 1999).

Because of the (near) constancy of the opening angle, the writhe decreases significantly with increasing packing fraction through the phase transition. According to the fact that through White's Eq. 1 the sum of the excess twist and the writhe are conserved (White, 1969), this decrease in writhe should be compensated by a positive twist exerted on the DNA duplex if the linking number deficit is fixed. With the results in Table 1, the excess twist should increase by approximately eight turns if the concentration is increased from 3 to 27 g of DNA/dm^3. This increase in ΔTw corresponds to a twist of ~1° per base pair, and with a torsional persistence length $L_t \approx 75$ nm (Bloomfield et al., 2000), the associated free energy amounts ~0.04 kT. If the twist exceeds a certain critical value, the torsion may be (partially) relaxed with the phosphate backbone turned inside and the unpaired bases exposed on the outside (Strick et al., 1998). We found, however, no evidence for this effect, because the cross-sectional radius of gyration of the duplex agrees with the B form for all investigated plasmid concentrations. It is our conjecture that the free energy associated with the excess twist is of paramount importance in controlling the critical boundaries pertaining to the transition to the liquid crystalline phase.

Another possibility for an increase in number of superhelical turns is an ionic strength induced decrease in helical repeat distance of the double-stranded DNA duplex. Cherny and Jovin (2001) observed a change of configuration of negatively supercoiled pPGM1 plasmid (2987 bp) from a plectonemic form with one or two nodes to 14 ± 1 nodes, if the concentration of monovalent salt is increased from −0.001 to 0.05 M. For high salt concentration, the number of nodes approached the expected value for a 3000 bp plasmid with a superhelical density $\sigma \sim -0.06$. In our situation, the number of nodes (which is on the order of minus the writhe) increases *beyond* the expected value ~7 ($\sigma \sim -0.03$) to ~18 with an increase in ionic strength from 0.05 to 0.06 M (the increase in ionic strength comes from uncondensed counterions only). Because such a significant effect from such a small increase in ionic strength is unlikely, we consider a change in helical repeat distance of the duplex irrelevant in explaining the observed change in overall DNA geometry.

For a rigid rod with length L and diameter D, the second virial coefficient including end effects reads $A_2 = \pi/4\, L^2\, D(1 + 4\, D/L)$ (Onsager, 1949; Odijk, 1990). With the normalized lengths and second virial coefficients in Table 1, we derive an effective diameter pertaining to the excluded volume $D = 4$, 9, and 15 nm for 6, 11, and 27 g of DNA/dm^3, respectively. The latter values are on the same order of magnitude as twice the plectonemic radius (Table 1), which shows that the supercoils take indeed a rather extended configuration. However, because no good models are available to describe the excluded volume of supercoiled DNA, including the effects of branching and overall flexibility, we consider further interpretation of A_2 not feasible.

CONCLUSIONS

With a view to determine the configuration and regularity of plectonemically supercoiled DNA, we have measured the small angle neutron scattering from pUC18 plasmid in 0.05 M NaCl. In the present q range, interference over a spatial extent on the order of the radius and pitch of the supercoil

is sampled and, accordingly, effects of overall flexibility and/or branching of the superhelix are beyond observation. We have derived the mathematical expression for the single chain scattering function (form factor) of an interwound structure. In particular, for a precise estimate of the superhelical dimensions and to ensure the correct high q limiting behavior of the structure factor, it appeared to be necessary to include the longitudinal interference over the plectonemic pitch. Interactions among supercoils can be taken into account in the second virial approximation, because at the present ionic strength electrostatic interactions are screened over a spatial extent less than the superhelical diameter. It was found that a *local* plectonemic structure describes the scattering data well, provided a significant distribution in radius and pitch is included. This distribution comes from a variation in molecular shape resulting from a distribution in linking number deficit and/or thermal fluctuations. Furthermore, the partitioning of DNA over coexisting isotropic and liquid crystalline phases with a concomitant change in plectonemic dimensions contributes to a broadening of the distribution in radius. We have assumed that the plectonemic opening angle is constant, so that the variation in pitch is correlated with the one in radius. A model in which the pitch and radius are allowed to fluctuate independently gives an inferior fit to the data. Furthermore, we would not be able to detect a modest fluctuation in opening angle, because theoretical analysis shows that this gives a minor additional damping of the normalized structure factor only.

For diluted supercoils with vanishing mutual interaction, the derived results for the radius, pitch, opening angle, and normalized length agree with independent electron microscopy measurements by Boles et al. (1990), scanning force microscopy (Rippe et al., 1997), and previous SANS work (Torbet and DiCapua, 1989; Hammermann et al., 1998). Furthermore, the estimated number of superhelical turns (proportional to minus the writhing number), as well as the variation, agrees with the linking number deficit as determined by gel electrophoresis. This suggests that the main contribution to the variation in adjusted parameters comes from the presence of a distribution in topoisomers rather than thermal fluctuations. However, to gauge the relative importance of the fluctuation contribution it is necessary to do experiments with a narrow distribution in preset linking number deficit. With increasing plasmid concentration, prior and covering the transition to a liquid-crystalline phase, the radius and pitch are seen to decrease significantly. The opening angle and normalized length show a slight tendency to decrease as well, but they remain relatively close to the average values 58° and 0.85°, respectively. The latter observation implies that compaction of negatively supercoiled DNA by spatial confinement results in a decrease in writhing number at the cost of a positive twist exerted on the DNA duplex. It is our conjecture that the free energy associated with this excess twist is of paramount importance in controlling the critical boundaries pertaining to the transition to the anisotropic, liquid-crystalline phase.

APPENDIX: FORM FACTOR OF A REGULAR PLECTONEMIC COIL

For the calculation of the form factor, the DNA supercoil is placed with its central axis along the z axis in a coordinate system with rectangular unit vectors **i**, **j**, and **k** (Fig. 8). It is assumed that the two strands of the superhelix are diametrically arranged in the xy plane such that they are always exactly opposite each other. A point on strand $\pm$ is hence described by position vector

$$\mathbf{s}_{\pm} = \pm r\cos(z/p)\mathbf{i} \pm r\sin(z/p)\mathbf{j} + z\mathbf{k} \qquad (10)$$

with z the projected distance on the helical axis. The momentum transfer vector **q** is expressed in the spherical coordinates q, θ, and φ, so that

$$\mathbf{q}\cdot\mathbf{s}_{\pm} = q\mu z \pm qr(1-\mu^2)^{1/2}\cos(\varphi - z/p) \qquad (11)$$

with $\mu = \cos\theta = \mathbf{q}\cdot\mathbf{k}/q$. With Eq. 11, the scattering amplitude ρ_q (with complex conjugate ρ_q^*) takes the form

$$\rho_q = \frac{1}{L}\int_{-L/2}^{L/2} dz(\exp(i\mathbf{q}\cdot\mathbf{s}_+) + \exp(i\mathbf{q}\cdot\mathbf{s}_-))/2$$

$$= \frac{1}{L}\int_{-L/2}^{L/2} dz\,\exp(iq\mu z)\cos(qr(1-\mu^2)^{1/2}\cos(\varphi - z/p)) \qquad (12)$$

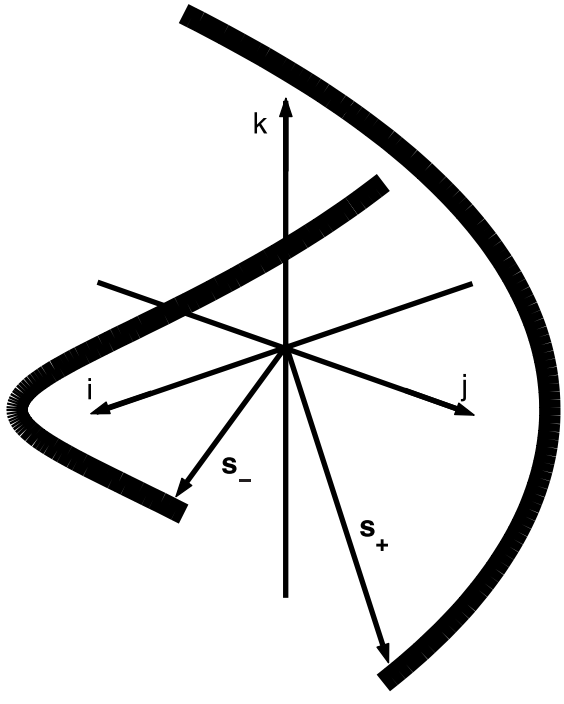

FIGURE 8 Coordinate system describing the position vectors s_+ and s_- of the two opposing strands in the superhelix.

To facilitate the integrations, we express Eq. 12 in the associated series of the Bessel functions of integer order J_k (Abramowitz and Stegun, 1970)

$$\rho_q = \frac{1}{L}\int_{-L/2}^{L/2} dz\, \exp(iq\mu z)\Big[J_0(qr(1-\mu^2)^{1/2}) + 2\sum_{k=1}^{\infty}(-)^k J_{2k}(qr(1-\mu^2)^{1/2})\cos(2k(\varphi - z/p))\Big] \quad (13)$$

in which the restriction to the even $2k$ terms comes from the fact that the contributions of the two opposing strands have been averaged. The integration over z is readily done:

$$\rho_q = \frac{\sin(q\mu L/2)}{(q\mu L/2)} J_0(qr(1-\mu^2)^{1/2}) + 2\sum_{k=1}^{\infty}(-)^k J_{2k}(qr(1-\mu^2)^{1/2}) C_{2k}(\mu, \varphi) \quad (14)$$

with the orientation dependent coefficients

$$C_k(\mu, \varphi) = \frac{2p}{L((q\mu p)^2 - k^2)}\left(\cos\left(\frac{kL}{2p}\right)\sin\left(\frac{q\mu L}{2}\right) \times (q\mu p\cos(k\varphi) + ik\sin(k\varphi)) - \sin\left(\frac{kL}{2p}\right)\cos\left(\frac{q\mu L}{2}\right)(k\cos(k\varphi) + iq\mu p\sin(k\varphi))\right) \quad (15)$$

It can easily be shown that the latter coefficients satisfy the orthogonality relationships

$$\frac{1}{2\pi}\int_0^{2\pi} d\varphi C_k(\mu, \varphi) = 0 \quad (16)$$

$$\frac{1}{2\pi}\int_0^{2\pi} d\varphi C_k(\mu, \varphi) C_m^*(\mu, \varphi) = 0\,, \quad k \neq m \quad (17)$$

$$\frac{1}{2\pi}\int_0^{2\pi} d\varphi C_k(\mu, \varphi) C_k^*(\mu, \varphi) = \left(\frac{\sin((q\mu + k/p)L/2)}{(q\mu + k/p)L}\right)^2 + \left(\frac{\sin((q\mu - k/p)L/2)}{(q\mu - k/p)L}\right)^2 \quad (18)$$

The general expression of the form factor reads

$$P(q) = \langle \rho_q \rho_q^* \rangle \quad (19)$$

in which the brackets denote an isotropic orientation average of the momentum transfer vector with respect to the supercoil:

$$\langle \cdots \rangle = \int_0^1 d\mu \frac{1}{2\pi}\int_0^{2\pi} d\varphi \cdots \quad (20)$$

(Lovesey, 1984). With the orthogonality relationships Eqs. 16, 17, and 18, the exact form factor pertaining to a regular plectonemic structure can now be calculated and reads

$$P(q) = \int_0^1 d\mu \Bigg(\left[\frac{\sin(q\mu L/2)}{(q\mu L/2)}\right]^2 J_0^2(qr(1-\mu^2)^{1/2}) + \sum_{k=1}^{\infty}\Bigg(\left[\frac{\sin((q\mu + 2k/p)L/2)}{(q\mu + 2k/p)L/2}\right]^2 + \left[\frac{\sin((q\mu - 2k/p)L/2)}{(q\mu - 2k/p)L/2}\right]^2\Bigg) J_{2k}^2(qr(1-\mu^2)^{1/2})\Bigg) \quad (21)$$

The integration over the orientation variable μ has to be done numerically.

In the long wavelength limit $q \to 0$, the form factor can be expressed in powers of q. Up to and including the second moment of the mass distribution, we get

$$P(q) = 1 - R_g^2 q^2/3 + \cdots \quad (22)$$

with the radius of gyration of the elongated supercoil without end loops defined by

$$R_g^2 = (L^2 + 12r^2)/12 \quad (23)$$

Due to the open core of the superhelix, the radius of gyration differs slightly from the one pertaining to a uniform rod given by $R_g^2 = (L^2 + 6r^2)/12$ (Higgins and Benoit, 1994).

In our range of momentum transfer, local structure is probed with $qL \gg 1$ and the form factor can considerably be simplified. The dominant contributions to the integral in Eq. 21 come from $\mu = 0$ and $\mu = 2k/(qp)$ for the terms proportional to J_0^2 and J_{2k}^2, respectively. Accordingly, to a very good approximation, we can substitute $\mu = 0$ and $\mu = 2k/(qp)$ in the arguments of J_0 and J_{2k}, respectively, and shift the corresponding terms in front of the integration signs (*i.e.*, we ignore their dependence on μ). Furthermore, the summation index k is confined to $k < qp/2$, because the orientation variable $\mu = 2k/(qp) = \mathbf{q}\cdot\mathbf{k}/q$ is in the range $0 \le \mu \le 1$. With these approximations, the form factor reads

$$P(q) = J_0^2(qr)\int_0^1 d\mu\left[\frac{\sin(q\mu L/2)}{(q\mu L/2)}\right]^2 + \sum_{k=1}^{qp/2} J_{2k}^2((q^2 - 4k^2/p^2)^{1/2} r) \times \int_0^1 d\mu\Bigg(\left[\frac{\sin((q\mu + 2k/p)L/2)}{(q\mu + 2k/p)L/2}\right]^2 + \left[\frac{\sin((q\mu - 2k/p)L/2)}{(q\mu - 2k/p)L/2}\right]^2$$

$$= \frac{2}{qL}\Bigg[J_0^2(qr)\int_0^{qL/2} dx[\sin x/x]^2 + \sum_{k=1}^{qp/2} J_{2k}^2((q^2 - 4k^2/p^2)^{1/2} r) \times \int_{kL/p - qL/2}^{kL/p + qL/2} dx[\sin x/x]^2\Bigg] \quad (24)$$

Finally, for $qL \gg 1$ the nonzero integration limits can be replaced by $\pm\infty$ and with $\int_0^\infty dx(\sin x/x)^2 = \pi/2$ the form factor reduces to the relatively simple form

$$P(q) = \frac{\pi}{qL}\left[J_0^2(qr) + 2\sum_{k=1}^{qp/2} J_{2k}^2((q^2 - 4k^2/p^2)^{1/2}\, r)\right], \quad qL \gg 1 \quad (25)$$

We thank Jacky Snoep, Coen van der Weijden, Hans den Dulk, and Tineke de Ruijter for technical support and assistance with gel electrophoresis and biochemical preparation procedures. Job Ubbink, Floske Spieksma, Don Woessner, Hans Westerhoff, and Victor Bloomfield are gratefully acknowledged for stimulating discussions. We acknowledge the Laboratoire Léon Brillouin and the Institut Max von Laue - Paul Langevin in providing the neutron research facilities.

REFERENCES

Abramowitz, M., and I. A. Stegun. 1970. Handbook of Mathematical Functions. Dover, New York.

Backendorf, C., R. Olsthoorn, and P. van de Putte. 1989. Superhelical stress restrained in plasmid DNA during repair synthesis initiated by the UvrA, B-protein and C-proteins in vitro. *Nucleic Acids Res.* 17: 10337–10351.

Bates, A. D., and A. Maxwell. 1993. DNA Topology. Oxford University Press, Oxford.

Bednar, J., P. Furrer, A. Stasiak, J. Dubochet, E. H. Egelman, and A. D. Bates. 1994. The twist, writhe and overall shape of supercoiled DNA change during counterion-induced transition from a loosely to a tightly interwound superhelix: possible implications for DNA structure in vivo. *J. Mol. Biol.* 235:825–847.

Bhikhabhai, R., M. Ollivier, and F. Blanche. 2000. A novel, rapid process for purification of plasmid for gene therapy. *Life Sci. News.* 5:1–4.

Bloomfield, V. A., D. M. Crothers, and I. Tinico, Jr. 2000. Nucleic Acids, Structures, Properties, and Functions. University Science Books, Sausalito.

Boles, T. C., J. H. White, and N. R. Cozzarelli. 1990. Structure of plectonemically supercoiled DNA. *J. Mol. Biol.* 213:931–951.

Brady, G. W., D. B. Fein, H. Lambertson, V. Grassian, D. Foos, and C. J. Benham. 1983. X-ray scattering from the superhelix in circular DNA. *Proc. Nat. Acad. Sci. U.S.A.* 80:741–744.

Brady, G. W., M. Satkowski, D. Foos, and C. J. Benham. 1987. Environmental influences on DNA superhelicity: the effect of ionic strength on superhelix conformation in solution. *J. Mol. Biol.* 195:186–191.

Cherny, D. I, and T. M. Jovin, 2001. Electron and scanning force microscopy studies of alterations in supercoiled DNA tertiary structure. *J. Mol. Biol.* 313:295–307.

de Gennes, P. G. 1979. Scaling Concepts in Polymer Physics. Cornell University Press, Ithaca.

des Cloiseaux, J., and G. Jannink. 1990. Polymers in Solution: Their Modelling and Structure. Clarendon Press, Oxford.

Fixman, M., and J. Skolnick. 1978. Polyelectrolyte excluded volume paradox, *Macromolecules.* 11:863–867.

Fujimoto, B. S., and J. M. Schurr. 2002. Monte Carlo simulations of supercoiled DNAs confined to a plane. *Biophys. J.* 82:944–962.

Gebe, J. A., J. J. Delrow, P. J. Heath, B. S. Fujimoto, D. W. Stewart, and J. M. Schurr. 1996. Effects of Na^+ and Mg^{2+} on the structures of supercoiled DNAs: comparison of simulations with experiments. *J. Mol. Biol.* 262:105–128.

Hammermann, M., N. Brun, K. V. Klenin, R. May, K. Toth, and J. Langowski. 1998. Salt-dependent DNA superhelix diameter studied by small angle neutron scattering measurements and Monte-Carlo simulations. *Biophys. J.* 75:3057–3063.

Higgins, J. S., and H. C. Benoit. 1994. Polymers and Neutron Scattering. Clarendon Press, Oxford.

Jacrot, B. 1976. The study of biological structures by neutron scattering from solution. *Rep. Prog. Phys.* 39:911–953.

Klenin, K., H. Merlitz, and J. Langowski. 1998. A Brownian dynamics program for the simulation of linear and circular DNA and other wormlike chain polyelectrolytes. *Biophys. J.* 74:780–788.

Lovesey, S. W. 1984. Theory of Neutron Scattering from Condensed Matter, Vol. 1. Oxford University Press, Oxford.

Lyubchenko, Y. L., and L. S. Shlyakhtenko. 1997. Visualization of supercoiled DNA with atomic force microscopy in situ. *Proc. Natl. Acad. Sci. U.S.A.* 94:496–501.

Manning, G. S. 1969. Limiting laws and counterion condensation in polyelectrolyte solutions: I. Colligative properties. *J. Chem. Phys.* 51: 924–933.

Marko, J. F., and E. D. Siggia. 1995. Statistical-mechanics of supercoiled DNA. *Phys. Rev. E.* 52:2912–2938.

Nierlich, M., C. E. Williams, F. Boué, J. P. Cotton, M. Daoud, B. Farnoux, G. Jannink, C. Picot, M. Moan, C. Wolff, M. Rinaudo, and P. G. de Gennes. 1979. Small angle neutron scattering by semi-dilute solutions of polyelectrolyte. *J. Phys. Fr.* 40:701–704.

Norisuye, T., H. Murakama, and H. Fujita. 1978. Wormlike chains near the rod limit: moments and particle scattering function. *Macromolecules.* 11:966–970.

Odijk, T. 1990. Electrostatic interactions in a solution of linear micelles. *J. Chem. Phys.* 93:5172–5176.

Onsager, L. 1949. The effects of shape on the interaction of colloidal particles. *Ann. N.Y. Acad. Sci.* 51:627–659.

Prazeres, D. M. F., T. Schluep, and C. Cooney. 1998. Preparative purification of supercoiled plasmid DNA using anion-exchange chromatography. *J. Chromatogr. A.* 806:31–45.

Reich, Z., E. J. Wachtel, and A. Minsky. 1994. Liquid-crystalline mesophases of plasmid DNA in bacteria. *Science.* 264:1460–1463.

Rippe, K., N. Mucke, and J. Langowski. 1997. Superhelix dimensions of a 1868 base pair plasmid determined by scanning force microscopy in air and in aqueous solution. *Nucleic Acids Res.* 25:1736–1744.

Rybenkov, V. V., A. V. Vologodskii, and N. R. Cozzarelli. 1997a. The effect of ionic conditions on the conformations of supercoiled DNA: I. Sedimentation analysis. *J. Mol. Biol.* 267:299–311.

Rybenkov, V. V., A. V. Vologodskii, and N. R. Cozzarelli. 1997b. The effect of ionic conditions on the conformations of supercoiled DNA: II. Equilibrium catenation. *J. Mol. Biol.* 267:312–323.

Stigter, D. 1977. Interactions of highly charged colloidal cylinders with applications to double-stranded DNA. *Biopolymers.* 16:1435–1448.

Strick, T. R., J. F. Allemand, D. Bensimon, and V. Croquette. 1998. Behavior of supercoiled DNA. *Biophys. J.* 74:2016–2028.

Sun, N., B. Chen, J. Zhou, J. Yuan, X. Xu, D. Zhu, and K. Han. 1994. An efficient method for large-scale isolation of plasmid DNAs by heat-alkali co-denaturation. *DNA Cell Biol.* 13:83–86.

Torbet, J., and E. DiCapua. 1989. Supercoiled DNA is interwound in liquid-crystalline solutions. *EMBO J.* 8:4351–4356.

Ubbink, J., and T. Odijk. 1999. Electrostatic-undulatory theory of plectonemically supercoiled DNA. *Biophys. J.* 76:2502–2519.

van der Maarel, J. R. C. 1999. Effect of spatial inhomogeneity in dielectric permittivity on DNA double layer formation. *Biophys. J.* 76:2673–2678.

van der Maarel, J. R. C., L. C. A. Groot, M. Mandel, W. Jesse, G. Jannink, and V. Rodriguez. 1992. Partial and charge structure functions of monodisperse DNA fragments in salt free aqueous solution. *J. Phys. II Fr.* 2:109–122.

van der Maarel, J. R. C., and K. Kassapidou. 1998. Structure of short DNA fragment solutions. *Macromolecules.* 31:5734–5739.

van Workum, M., S. J. M. van Dooren, N. Oldenburg, D. Molenaar, P. R. Jensen, J. L. Snoep, and H. V. Westerhoff. 1996. DNA supercoiling depends on the phosphorylation potential in *Escherichia coli*. *Mol. Microbiol.* 20:351–360.

White, J. H. 1969. Self-linking and the Gauss integral in higher dimensions. *Am. J. Math.* 91:693–728.

Yethiraj, A., and C.-Y. Shew. 1996. Structure of polyelectrolyte solutions. *Phys. Rev. Lett.* 77:3937–3940.

Zakharova, S. S., S. U. Egelhaaf, L. B. Bhuiyan, C. W. Outhwaite, D. Bratko, and J. R. C. van der Maarel. 1999. Multivalent ion-DNA interaction; neutron scattering estimates of polyamine distribution. *J. Chem. Phys.* 111:10706–10716.